PNC-TN9410 88-090

17

DROPLET DEPOSITION AND ENTRAINMENT MODELING BASED ON THE THREE-FLUID MODEL

August, 1988

OARAI ENGINEERING CENTER

POWER REACTOR AND NUCLEAR FUEL DEVELOPMENT CORPORATION

複製又はこの資料の入手については，下記にお問い合わせください。
〒311-13　茨城県東茨城郡大洗町成田町4002
動力炉・核燃料開発事業団
大洗工学センター　システム開発推進部・技術管理室

Enquires about copyright and reproduction should be addressed to: Technology Management Section O-arai Engineering Center, Power Reactor and Nuclear Fuel Development Corporation 4002 Narita-cho, O-arai-machi, Higashi-Ibaraki, Ibaraki-ken, 311-13, Japan

動力炉・核燃料開発事業団（Power Reactor and Nuclear Fuel Development Corporation）

PNC-TN9410 88-090
Aug. 1988

DROPLET DEPOSITION AND ENTRAINMENT MODELING BASED ON THE THREE-FLUID MODEL(*)

Satoru Sugawara(**)

ABSTRACT

General droplet deposition and entrainment models were developed. Validation studies of the models were also carried out using an analysis code FIDAS based on the three-fluid model. The models were tested on the flow rates of entrainment and liquid film for the adiabatic annular mist flow. The capability of the models were successfully demonstrated by comparisons between calculations and measurements of Hewitt et al. and Keeys et al. in AERE Harwell and of Wurtz in RISO and so on.

(*) To be presented to the Third International Topical Meeting on Nuclear Power Plant Thermal Hydraulics and Operations, November 14-17, Seoul, KOREA.

(**) Reactor Engineering Section, Safety Engineering Division, PNC-OEC.

CONTENTS

1. INTRODUCTION

The subchannel analysis is a useful mean for the prediction of dryout in rod bundles. In the subchannel analysis, there are two important processes; one is to predict correctly the distribution of steam quality and mass velocity etc. in subchannels, the other is to predict the dryout precisely based on the calculated quantities in subchannels. For the later, so far, empirical correlations have been mainly used. In consequence of this, an available range is limited only within experimental conditions, and the capability of these correlation in extrapolation is uncertain. Therefore, recently, some studies have been reported on the analytical prediction of dryout on the basis of annular flow model and 'the film dryout criterion' [1][2][3]. However, obtained results were insufficient to be applied for practical purpose, since no reliable models are given for the droplet entrainment and deposion which play most important role in the analytical prediction of dryout[4].

Thus, the objectives of this study are to develop further reliable models on the droplet entrainment and deposition in order to improve the prediction accuracy in the film dryout analysis, and to verify these models by comparing the experiments conducted at Atomic Energy Research Establishment (AERE) in Harwell, at Kyoto University and at RISO National Laboratory, which give data of flow rates of liquid film and entrainment in adiabatic annular mist flow.

In this study, the experiments are simulated with an analysis code FIDAS applying the full continuity and momentum conservation equations to the three fluids, namely, liquid film, liquid droplets and vapor core.

2. THE FIDAS CODE

The Film Dryout Analysis Code in Subchannels (FIDAS) has been developed by the author in Power Reactor and Nuclear Fuel Development Corporation (PNC) with a main objective of predicting the dryout and post-dryout heat transfer in rod bundles. FIDAS code provides a three-fluid, three-field representation of two-phase flow in a channel or rod bundle. The three fields are specified by continuous liquid film, continuous vapor and entrained liquid droplets suspended in the vapor. The code is generally formulated to be applicable to the wide range of hydraulic condition, especially to non-thermal-equilibrium transient conditions. Thus the basic 12 field equations consist of three continuity, three energy, six momentum equations. In the present study, however, only 9 field equations are used because a one-dimensional analysis is attempted. The 9 field equations together with the volume fraction conservation relation among three fields enable solution for the following 10 parameters : the three velocities, the three volume fractions, the three specific enthalpies, and the pressure. The field equations are given in Table 1.

The following constitutive equations are provided in the code.

(a) Droplet entrainment rate.
(b) Droplet deposition rate.
(c) Wall shear stress, between wall and liquid film in pre-dryout region, and between wall and vapor in post-dryout region.
(d) Vapor-liquid and vapor droplet interfacial drag forces.
(e) Droplet size.
(f) Convective heat transfer, between wall and liquid film in pre-dryout region, between wall and vapor in post-dryout region, and between wall and droplet in post-dryout region.
(g) Radiative heat transfer, between wall and vapor, and wall and droplet.
(h) Vapor-liquid and vapor-droplet interfacial heat transfer.
(i) Interfacial mass transfer, by condensation and vaporization.

The constitutive equations used in this study are summarized in Table 2. The interfacial shear stress between liquid film and vapor is estimated by Wallis'[5] correlation, besides, the wall shear stress and drag force of droplet are given by conventional single phase correlations. Moreover, the average droplet diameter is determined by the critical Weber number.

The computational scheme used is based on a semi-implicit method. The finite-difference equations obtained are linearized by means of Taylor's expansion, and the linear finite-difference matrix equations are solved using the Skyline solver. The specifications for boundary conditions are the inlet velocity (or mass flux), inlet temperature (or enthalpy), heat flux to the wall and the outlet pressure.

3. DEVELOPMENT OF DEPOSITION AND ENTRAINMENT MODELS

3.1 PREVIOUS WORKS

A number of experiments and correlations have been reported for the droplet deposition and entrainment[9]-[18]. These data and correlations were previously reviewed by Hewitt and Hall-Taylor[6], Kataoka and Ishii[7], and Ueda[8] and so on.

The deposition of droplets is usually expressed by a droplet deposion coefficient k_D. For this coefficient, Paleev et al.[9], Whalley[1], Bennett et al.[10], and Saito[2] gave various correlations.

Paleev et al. derived following correlation from his experimental data on the basic of diffusion mechanism.

$$\frac{k_D}{u_G} = 0.022\ Re_G^{-0.25} \left(\frac{C}{\rho_G} \right)^{-0.26} . \qquad (1)$$

Since his experimental data limited in atmospheric air-water flow, it is doubtful that the correlation can apply directly to the high pressure steam-water flow. Whalley recommended a tentative correlation of k_D in term of interfacial tension. Besides bennett et al. and Saito correlated k_D as a function of the droplet concentration. However, it is questionable that a complex phenomenon like the droplet deposition could be correlated as a function of only the interfacial tension or droplet concentration.

As for the droplet entrainment rate m_E, Huchinson and Whalley[15], Ueda[16], and Kataoka and Ishii[7] provided representative expressions.

Hutchinson and Whalley attempt to correlate entrainment data as a function of dimensionless parameter ($\tau_{FG}\delta_F/\sigma$) based on the force balance at the wavy interface between liquid film and vapor. However, the data showed considerable scattering in the comparison with the correlation.

Ueda presented the correlation in a similar manner as the above mentioned correlation developed by Huchinson and Whalley.

$$m_E = 3.54\times 10^{-3}\left[\left(\frac{\tau_{FG}}{\sigma}\right)\left(\frac{u_F\alpha_F}{\sigma}\right)^{0.6}\right]^{0.57}, \qquad (2)$$

$$\text{for}\quad \left(\frac{\tau_{FG}}{\sigma}\right)\left(\frac{u_F\alpha_F}{\sigma}\right)^{0.6} \geqq 120 \quad . \qquad (3)$$

Although Eq.(2) correlates his experimental data, a parameter $(\tau_{FG}/\sigma)\,(u_F\alpha_F/\sigma)^{0.6}$ is dimensional and not based on physical mechanism of entrainment. Therefore, it seems that the correlation may not be available in general cases.

Kataoka and Ishii proposed a further detailed following correlation on the basis of entrainment inception criteria and force balance at the wavy interface.

For under entrained regime($Re_{ff} \geqq Re_{ff}^{\infty}$)

$$\frac{m_E\cdot D_h}{\mu} = 1.2\times 10^{3}Re_f^{-0.5}Re_{ff}^{\infty\,-0.25}We^{-1.5}(Re_{ff}-Re_{ff}^{\infty})^2 + 6.6\times 10^{-7}Re_f^{0.74}Re_{ff}^{0.185}We^{0.925}\left(\frac{\mu_G}{\mu_F}\right)^{0.26} . \qquad (4)$$

For over entrained regime ($Re_{ff} < Re_{ff}^{\infty}$)

$$\frac{m_E\cdot D_h}{\mu} = 6.6\times 10^{-7}Re_f^{0.74}Re_{ff}^{0.185}We^{0.925}\left(\frac{\mu_G}{\mu_F}\right)^{0.26}, \qquad (5)$$

where
$Re_{ff} = Re_f(1-E)$,
$Re_{ff}^{\infty} = Re_f(1-E^{\infty})$,
$E^{\infty} = \tanh(7.25\times 10^{-7}We^{1.25}Re_f^{0.25})$.

Since this correlation was adjusted with the limited experimental

data in atmospheric air-water flow, it is expected that the correlation may not apply directly to general cases, and that prediction accuracy may deteriorate in high steam quality region where the fraction of film flow decreases, because they apply the hyperbolic tangent function to correlate the equilibrium amount of droplet.

The above mentioned situation suggests that existing correlations for droplet deposition and entrainment are unsatisfactory for predicting the dryout on the basic of 'the film dryout criterion' in high pressure steam-water two-phase flow.

3.2 DERIVATION OF A DROPLET DEPOSITION MODEL

In the annular two-phase flow, turbulent diffusion is a dominant mechanism of the droplet deposition onto liquid film [22]. In view of this, the present model is developed based on the turbulent diffusivity of entrained droplets in the vapor core.

The normal empirical relationship for heat transfer in turbulent flow is that of Colburn[21] and is as follows.

$$Nu = \frac{hD}{\lambda} = 0.023\ Re_G^{0.8}\ Pr^{1/3} \quad . \qquad (6)$$

Considering the analogous between mass transfer and heat transfer, Eq.(6) can be rewritten by

$$Sh = \frac{k_G D}{D_G} = 0.023 \left(\frac{u_G D}{\nu_G} \right)^{0.8} \left(\frac{\nu_G}{D_G} \right)^{1/3}$$

$$= 0.023\ Re_G^{0.8}\ Sc^{1/3} \quad . \qquad (7)$$

If $k_G=k_D$ is assumed, Eq.(7) becomes

$$\frac{k_D}{u_G} = 0.023 \left(\frac{u_G D}{\nu_G} \right)^{-0.2} \left(\frac{D_G}{\nu_G} \right)^{2/3}$$

$$= 0.023 \, Re_G^{-0.2} \, Sc^{-2/3} \quad . \tag{8}$$

Bennett et al.[10] found out that the deposition coefficient k_D is affected by the droplet concentration in vapor core. Bennett presumed that high droplet concentration will lead to a modification of the drift velocity of droplet towards the film surface, and that the droplet will coalesce and respond less to the turbulence of the vapor core and finally the presence of droplet will damped the turbulence itself.

Therefore, taking into account the effect of droplet concentration, Eq.(8) is rewritten as follows.

$$\frac{k_D}{u_G} = f(C) \, Re_G^{-0.2} \, Sc^{-2/3} \quad , \tag{9}$$

where f(C) is the nondimensional Droplet concentration parameter. From this equation, f(C) can be expressed by

$$f(C) = \frac{k_D}{u_G} Re_G^{0.2} \, Sc^{2/3} \quad . \tag{10}$$

Figure 2 shows the value of f(C), in term of (C/ρ_G), determined by Eq.(10) from the various experiments. As is apparently seen in this figure, the deposition coefficient decreases with the increase in droplet concentration, and the experimental results obtained under different conditions can be

well correlated with a function expressed as follows.

$$f(C) = 9.0\times 10^{-3} \left(\frac{C}{\rho_G} \right)^{-0.5} . \qquad (11)$$

Finally, from Eq.(9) and Eq. (11), one can obtain the following new correlation for the droplet deposition coefficient.

$$\frac{k_D}{u_G} = 9.0\times 10^{-3} \left(\frac{C}{\rho_G} \right)^{-0.5} Re_G^{-0.2} Sc^{-2/3} , \qquad (12)$$

with,

$$C = \frac{W_E}{\frac{W_G}{\rho_G}\cdot\frac{u_E}{u_G} + \frac{W_E}{\rho_L}} . \qquad (13)$$

In this expression, Schmidt number is calculated using the Lewis' relation, i.e. Le≒ 1.

3.3 DERIVATION OF A DROPLET ENTRAINMENT MODEL

For low viscous fluid such as steam-water system, shearing off of roll wave crests dominates to entrain droplets into the vapor core of annular two-phase flow [6][7][8]. From the view point of this, the present model derivation is concentrated on the roll wave mechanism.

In order to get a new model applicable to a wide range of pressure from an atmospheric to reactor operating condition, an attempt was made to take into account the effects of density ratio between vapor and liquid film, and of hydrodynamic equivalent wave height. In particular, change in the density

ratio over the wide range of pressure is not negligible. Furthermore, the equivalent hydrodynamic wave height is considered to be dependent to the gas Reynolds number because shear stress at the wary interface affected by the gas Reynolds number.

It is denoted from the force balance at the crest of roll wave that the droplet entrainment occurs when the interfacial shear force exceeds the retaining force of liquid film.

The interfacial shear force at the crest of roll wave exerted by the streaming vapor flow is given by

$$F_{FG} = k_f \cdot \frac{\rho_G \cdot u_{GF}^2}{2} \cdot A_r \quad . \tag{14}$$

Since $A_r = \triangle h_{eq}$ and τ_{FG} $(k_f \cdot \rho_G \cdot u_{GF}^2/2)$ for the unit width, Eq.(14) is rewritten as

$$F_{FG} \quad \tau_{FG} \cdot \triangle h \quad . \tag{15}$$

On the other hand, the surface tension σ is considered as a dominant force of the retaining of roll waves and the hydrodynamic equivalent wave height $\triangle h_{eq}$ is more appropriate to express the shear force at roll wave than actual wave height. Therefore, substitution of σ with $\triangle h_{eq}$ in Eq.(15) gives the following dimensionless parameter.

$$S_1 = \frac{\tau_{FG} \cdot \triangle h_{eq}}{\sigma} \quad . \tag{16}$$

Introducing the dimensionless gas velocity ($u_G \cdot \mu_F/\sigma$) recommended by Wurtz[3] into the dimensionless parameter S_1, one

can revise the parameter S1 to the following dimensionless expression.

$$S_2 = \left(\frac{\tau_{FG} \cdot \triangle h_{eq}}{\sigma} \right) \left(\frac{u_G \cdot \mu_F}{\sigma} \right) \quad . \tag{17}$$

Furthermore, taking into account the effect of density ratio between liquid film and vapor, one can finally obtained the following new dimensionless parameter.

$$S_R = \left(\frac{\tau_{FG} \cdot \triangle h_{eq}}{\sigma} \right) \left(\frac{u_G \cdot \mu_L}{\sigma} \right) \left(\frac{\rho_F}{\rho_G} \right)^n \quad . \tag{18}$$

The experimental data of Hewitt et al.[19] and Keeys et al.[20] are plotted against S_2 in Fig.3, and against S_R in Fig.4. The comparison between Figs. 3 and 4 shows that the data can be satisfactorily correlated if n= 0.40. Hence, the final expression for m_E is given as follows.

$$\begin{aligned} m_E &= 1.07\ S_R \\ &= 1.07 \left(\frac{\tau_{FG} \cdot \triangle h_{eq}}{\sigma} \right) \left(\frac{u_G \cdot \mu_L}{\sigma} \right) \left(\frac{\rho_F}{\rho_G} \right)^{0.4} \quad . \end{aligned} \tag{19}$$

The value of $\triangle h_{eq}$ is assumed to be calculated by the following hydrodynamic equivalent wave roughness k_S recommended by Wurtz.

$$\begin{aligned} k_S = {} & 0.57\ t_F + 21.73 \times 10^3\ t_F^2 \\ & - 38.8 \times 10^6\ t_F^3 + 55.68 \times 10^9\ t_F^4 \quad . \end{aligned} \tag{20}$$

Although the effect of pressure on the entrainment rate can be well taken into account by introducing the effect of density ratio $(\rho_F/\rho_G)^{0.4}$, large discrepancy between the calculation by Eq.(19) and the experiments is recognized in Fig.4 especially for low pressure data. Probably, this discrepancy is due to unsuitable extrapolation of k_s, which estimated by Wurtz in the rather high pressure range of 3 to 9 MPa, to the atmospheric pressure.

In order to resolve this discrepancy, suitable values of Δh_{eq} were determined from the comparison between the calculated value by Eq.(19) and the experimental data, and plotted against the gas Reynolds number in Fig.5. The figure shows that the $\Delta h_{eq}/k_s$ is estimated significantly smaller than the value of k_s calculated by Eq.(20), and that hydrodynamic equivalent wave height proportionally decreases with decrease of the gas Reynolds number in the range of $Re_G<1\times10^5$. The same trend is recognized in Ueda's analysis[16] in lower gas velocity region. Accordingly, the hydrodynamic equivalent wave height Δh_{eq} should be correlated as a function of the gas Reynolds number.

Finally, from Eq.(19) and Fig.5, one can obtain the following new correlation of the droplet entrainment rate.

$$m_E = 1.07 \left(\frac{\tau_{FG}\cdot\Delta h_{eq}}{\sigma} \right)\left(\frac{u_G\cdot\mu_L}{\sigma} \right)\left(\frac{\rho_F}{\rho_G} \right)^{0.4} , \qquad (21)$$

$$\Delta h_{eq} = k_s \qquad (Re_G>1\times10^5), \qquad (22)$$

$$\Delta h_{eq} = k_s \left[2.136\log(Re_G) - 9.68 \right] \qquad (Re_G<1\times10^5), \qquad (23)$$

where $\Delta h_{eq} > 0.0$.

The comparisons between the values calculated by Eq.(21) and the experimental data of AERE Harwell are shown in Fig.6. This figure, shows that Eq.(21) is applicable to estimate the entrainment rates in a wide range of pressure and mass velocity.

4. CODE AND MODEL ASSESSMENTS

Several measurements of liquid film and entrained droplet flow rates in the adiabatic steam-water two-phase flow have been so for carried out and reported. The representatives are those by Hewitt et al.[19], Keeys et al.[20], Yanai[23] and Wurtz[3]. Experimental condition in these studies are summarized in Table 3. These experimental were applied to data validation study of the FIDAS code incorporating newly developed droplet entrainment and deposition correlations.

4.1 ANALYSIS FOR THE AERE EXPERIMENTS

The experiments were conducted by Hewitt et al.[19] in the pressure range of 0.24 to 0.45 MPa, and by Keeys et al.[20] in the pressure range of 3.45 to 6.89 MPa. The test sections used in the experiments have a same inside diameter of 9.2 mm, length of 1.83 and 3.66 m in Hewitt's experiment and of 3.66 m in Keeys' experiment. Sinter tubes were used as a mixing device and a film removal device.

In the analysis, it is necessary to give a proper value of initial entrainment fraction defined at the test section inlet defined as follows.

$$\alpha_{E,INI} = f\alpha_E (\alpha_E + \alpha_F) = f\alpha_E (1 - \alpha_G) \qquad (24)$$

However, no experimental information on $\alpha_{E,INI}$ are reported. Therefore, in advance of the validation analysis, a series of calculations were performed by changing $\alpha_{E,INI}$ parametrically until calculational results agree well with experimental ones for axial variation of entrained droplet flow rate measured by Hewitt et al. and for quasi-equilibrium droplet flow rate measured at the test section exit by Hewitt et al. and Keeys et al. These calculations show that a proper value of $\alpha_{E,INI}$ is 0.001, and fortunately calculation for the flow rates of liquid film and entrained droplets is insensitive to selection of $\alpha_{E,INI}$, especially in high steam quality region in the range of X_{ex}>50%.

Accordingly, the analyses for the AERE experiments were conducted on the assumption that $\alpha_{E,INI} = 0.001$.

Comparisons between analyses and experiments on the flow rates of liquid film and entrained droplet are shown in Fig.7 for the AERE low pressure experiment by Hewitt et al. As is clearly seen in the figure, the analysis agree well with the experiments in the dependence of entrained droplet and liquid film flow rates on the steam quality and system pressure. Similar comparisons are indicated in Fig.8 for the AERE high pressure experiment made by Keeys et al. The comparisons also show that the analysis trace well the experimental dependence of entrained droplet and liquid film flow rates on the pressure and mass velocity.

4.2 ANALYSIS FOR THE YANAI'S EXPERIMENT

Yanai[23] conducted the measurement of entrained droplet and liquid film flow rates in practically the same pressure, and in wider range of mass velocity compared with the AERE low pressure experiment. The test section used has a inside diameter of 12.0 mm, length of 2.30 m. The film removal device at the test section exit is fabicated from a sinter tube, and the mixing device is made from a 0.6 mm diameter multi-nozzle mixer.

Initial entrained droplet fraction $\alpha_{E,INI}$ at the inlet is also determined in advance of the analysis in the same way as in the analysis of AERE experiments. A proper value of $\alpha_{E,INI}$ is estimated as a $f\alpha_E$ is 0.5. This value of $\alpha_{E,INI}$ is larger than that used in the analysis of the AERE experiment. This seems to be caused by the difference in the structure of mixing device.

Comparisons between analysis and measurement are indicated in Fig.9 for the flow rates of liquid film and entrained droplet. The figure shows that analysis by the FIDAS code agrees well with the experiment.

4.3 ANALYSIS FOR WURTZ'S EXPERIMENT

Wurtz[3] carried out the measurement similar to those mentioned in the section of 4.1 and 4.2, in the range of pressure

from 3 to 9 MPa and range of mass velocity from 500 to 3000 kg/s.m^2. His experimental conditions are broader than those in the AERE high pressure experiment. Furthermore, two test sections which have different inside diameter of 10 and 20 mm are used. Although a structure of the mixing device was not described in his paper, fortunately, the analytical result is practically insensitive to adopted value of $\alpha_{E,INI}$ in the whole experimental range. This is due to the fact that the 9 m-long test section is so large that the equilibrium condition might be established. Accordingly, $\alpha_{E,INI}=0.001$ is used in the analysis for Wurtz's experiment.

The comparisons between analysis and experiment are shown in Fig. 10 for the liquid film flow rate, and in Fig.11 for the entrained droplets flow rate. These figures demonstrate that the analyses by FIDAS code trace well the effect of mass velocity and of test section diameter in the experimental results.

5. CONCLUSION

The new correlation for the droplet deposition was developed on the basis of turbulent diffusion mechanism. The correlation was formularized in the equation taking into account the effect of droplet concentration and Schmidt number. In addition, the correlation for the droplet entrainment was also developed based on the force balance at the gas-liquid wavy interface by taking into the effects of density ratio of vapor core and liquid film, and the effect of hydrodynamic equivalent wave height.

The validation analyses based on the experiments by Hewitt et al., Keeys et al., Yanai and Wurtz, show that the FIDAS code incorporated with the newly developed correlations has good capability in predicting the behavior of annular two-phase flow.

ACKNOWLEDGMENT

The author would like to express his appreciation to Dr. K.Shiba for his support of this research effort. The author thanks to Mr.H.Kato, Mr.N.Komatuzaki and Mr.K.Watanabe for the assistance in the analytical calculation.

NOMENCLATURE

A = axial cross-sectional area, m^2
A = average area between phases, m^2
A_r = axial cross-sectional area of roll wave, m^2
C = average droplet concentration, kg/m^3
D = diameter, m
D_G = diffusion coefficient, m^2/s
f = friction coefficient, dimensionless
G = mass velocity, $kg/s.m^2$
g = gravitational acceleration, m/s^2
H = specific enthalpy, J/kg
$\triangle h$ = wave height, m
K = coefficient in drag force expressions
k = mass transfer coefficient, m/s
k_s = equivalent wave roughness in Wurtz's model, m
L = axial length, m
m_D = deposition rate of droplets, $kg/s.m^2$
m_E = entrainment rate of droplets, $kg/s.m^2$
P = pressure, MPa
Pr = Prandtl number
Q = heat transfer rate, W/m^3
Re = Reynolds number
S = wetted perimeter on A, m
Sc = Schmidt number
Sh = Sherwood number
S_1, S_2, S_R = dimensionless parameter
t = time, s
t_F = mean film thickness, m
u = axial velocity, m/s
W = mass flow rate, kg/s
We = Weber number
x = steam quality, dimensionless
z = axial distance, m

Greek letters:

α = volume fraction, dimensionless
Γ = evaporation rate per unit volume, kg/s.m^3
ν = kinetic viscosity, m^2/s
ρ = density, kg/m^3
σ = surface tension, N/m
τ = shear stress, N/m^2
θ = angular position, degrees
μ = dynamic viscosity, kg/s. m

Subscripts:

C = referring to vapor core
E = referring to entrained droplets
eq = referring to equivalence
F = referring to liquid film
G = referring to gas core (vapor)
INI = referring to initial
r = referring to roll wave
T = referring to total
W = referring to the wall

REFERENCES

[1] Whalley, P.B.; "The Calculation of Dryout in A Rod Bundle", Int. J. of Multiphase Flow, 3(1977), 501-515.

[2] Saito, T., Hughes, E.D. and Carbon, M.W.; "Multi-Fluid Modeling of Annular Two-phase Flow", Nuclear Engineering & Design, 50(1978) 225-271.

[3] Wurtz, J.; "An Experimental and Theoretical Investigation of Annular Steam-Water Flow in Tubes and Annuli at 30 to 90 bar", RISO Report No.372 (1978).

[4] Owen, D.G. and Hewitt, G.F.; "A Proposed Entrainment Correlation", AERE-R-12279 (1986).

[5] Wallis, G.B.; "One-Dimensional Two-phase Flow", (McGraw-Hill,1969).

[6] Hewitt, G.F. and Hall-Taylor, N.S.; "Annular Two-Phase Flow", (Pergamon Press 1970).

[7] Kataoka, I. and Ishii, M.; "Mechanism and Correlation of Droplet Entrainment and Deposition in Annular Two-phase Flow", ANL-82-44 (1982).

[8] Ueda, T.; "A Gas-Liquid Two-Phase Flow : Hydrodynamics and Heat Transfer", (Yoken-do 1981). (in Japanese)

[9] Paleev, I.I. and Filippovich, B.S.; "Phenomena of Liquid Transfer in Two-phase Dispersed Annular Flow", Int. J. of Heat & Mass Transfer, 9 (1966) 1089.

[10] Bennett, A.W., Hewitt, G.F., Kearsey, H.A., Keeys, R.K.F. and Pulling, D.J.; "Studies of Burnout in boiling Heat Transfer to Water in Round Tubes with Non-Uniform Heating", AERE-R5076 (1966).

[11] Farmar, R., Grifith, P. and Rohsenow, W.M.; "Liquid Droplet Deposition in Two-Phase Flow", Trans. ASME, Ser.C, Vol.92, No.4 (1970) 587-594.

[12] Alexander, L.B. and Coldren, C.L.; "Droplet Transfer from Suspending Air to Duct Walls", Ind. Eng. Chem., 43-6 (1951) 1325.

[13] Cousins, L.B. and Hewitt, G.F.; "Liquid Mass Transfer in Annular Two-phase Flow : Droplet Deposition and Liquid Entrainment", AERE-R5657 (1968).

[14] Hewitt, G.F., Kearsey, H.A. and Keeys, R.K.F.; "Determination of Rate of Deposition of Droplets in A Heated Tube with Steam-Water Flow at 1000 psia", AERE-R6118 (1969).

[15] Whalley, P.B., Hewitt, G.F. and Huchinson, P.; "Experimental Wave and Entrainment Measurements in Vertical Annular Two-Phase Flow", AERE-R7521 (1973).

[16] Ueda, T.; "Droplet Entrainment Rate and Droplet Diameter in Annular Two-Phase Flow", Journal of JSME, Vol.45 No.389 (1979) 127-135.

[17] Whalley, P.B.; "Calculation of Entrainment in Annular Flow", AERE-M2555 (1972).

[18] Whalley, P.B. and Hewitt, G.F.; "The Correlation of Liquid Entrainment Fraction and Entrainment Rate in Annular Two Phase Flow", AERE-R9187 (1978).

[19] Hewitt, G.F. Pulling, D.J.; "Liquid Entrainment in Adiabatic Steam-Water Flow", AERE-R-5374 (1969).

[20] Keeys, R.K.F., Ralph, J.C. and Roberts, D.N.; "Liquid Entrainment in Adiabatic Steam-Water Flow at 500 and 1000 p.s.i.a.", AERE-R6293 (1970).

[21] Colburn, A.P.; Trans. AIChE, 29, 174, 1933.

[22] Sekoguchi, K.; "Progress of Heat Transfer Engineering : Gas-Liquid Two-Phase Flow", (Yoken-do, 1973). (in Japanese)

[23] Yanai, M; "Study on Boiling Heat Transfer in A Channel", PhD. Thesis of Kyoto University (1971).

Table 1 Field Equations

Continuity Equations

for the steam:

$$\frac{\partial}{\partial t}(\alpha_G \rho_G) + \frac{1}{A}\frac{\partial}{\partial z}(\alpha_G \rho_G u_G A) = -\Gamma_F + \Gamma_E \quad ,$$

for the liquid film:

$$\frac{\partial}{\partial t}(\alpha_F \rho_F) + \frac{1}{A}\frac{\partial}{\partial z}(\alpha_F \rho_F u_F A) = -\Gamma_F + \frac{S}{A}(m_D - m_E) \quad ,$$

for the entrained droplet:

$$\frac{\partial}{\partial t}(\alpha_E \rho_E) + \frac{1}{A}\frac{\partial}{\partial z}(\alpha_E \rho_E u_E A) = -\Gamma_E - \frac{S}{A}(m_D - m_E) \quad ,$$

and,

$$\alpha_G + \alpha_F + \alpha_E = 1 \quad .$$

Momentum Equations

for the steam:

$$\frac{\partial}{\partial t}(\alpha_G \rho_G u_G) + \frac{\partial}{\partial z}(\alpha_G \rho_G u_G^2) = -\alpha_G \frac{\partial P}{\partial z} - \overline{A_{FG}}\tau_{FG} - \overline{A_{EG}}\tau_{EG}$$
$$- \overline{A_{WG}}\tau_{WG} + (\Gamma_{FG} u_F - \Gamma_{GF} u_G) + (\Gamma_{EG} u_E - \Gamma_{GE} - u_G)$$
$$- \alpha_G \rho_G g \cos\theta \quad ,$$

for the liquid film:

$$\frac{\partial}{\partial t}(\alpha_F \rho_F u_F) + \frac{\partial}{\partial z}(\alpha_F \rho_F u_F^2) = -\alpha_F \frac{\partial P}{\partial z} + \overline{A_{FG}}\tau_{FG} - \overline{A_{EF}}\tau_{EF}$$
$$- \overline{A_{WF}}\tau_{WF} - (\Gamma_{FG} u_F - \Gamma_{GF} u_G) + \frac{S}{A}(m_D u_E - m_E u_F)$$
$$- \alpha_F \rho_F g \cos\theta \quad ,$$

for the entrained droplet:

$$\frac{\partial}{\partial t}(\alpha_E \rho_E u_E) + \frac{\partial}{\partial z}(\alpha_E \rho_E u_E^2) = -\alpha_E \frac{\partial P}{\partial z} + \overline{A_{EG}}\tau_{EG} + \overline{A_{EF}}\tau_{EF}$$

$$- \overline{A_{WE}}\tau_{WE} - (\Gamma_{EG} u_E - \Gamma_{GE} u_G) - \frac{S}{A}(m_D u_E - m_E u_F)$$

$$- \alpha_E \rho_E g \cos\theta \quad .$$

Energy equations

for the steam:

$$\frac{\partial}{\partial t}(\alpha_G \rho_G H_G) + \frac{1}{A}\frac{\partial}{\partial z}(\alpha_G \rho_G H_G u_G A) = -P\frac{\partial \alpha_G}{\partial t} - \frac{P}{A}\frac{\partial}{\partial z}(\alpha_G u_G A)$$

$$+ \Gamma_{FG} H_{g,sat} - \Gamma_{GF} H_{\ell,sat} + \Gamma_{EG} H_{g,sat} - \Gamma_{GE} H_{\ell,sat} + Q_G \quad ,$$

for the liquid film:

$$\frac{\partial}{\partial t}(\alpha_F \rho_F H_F) + \frac{1}{A}\frac{\partial}{\partial z}(\alpha_F \rho_F H_F u_F A) = -P\frac{\partial \alpha_F}{\partial t} - \frac{P}{A}\frac{\partial}{\partial z}(\alpha_F u_F A)$$

$$- \Gamma_{FG} H_{g,sat} + \Gamma_{GF} H_{\ell,sat} + Q_F + \frac{S}{A}(m_D H_E - m_E H_F) \quad ,$$

for the entrained droplet:

$$\frac{\partial}{\partial t}(\alpha_E \rho_E H_E) + \frac{1}{A}\frac{\partial}{\partial z}(\alpha_E \rho_E H_E u_E A) = -P\frac{\partial \alpha_E}{\partial t} - \frac{P}{A}\frac{\partial}{\partial z}(\alpha_E u_E A)$$

$$- \Gamma_{EG} H_{g,sat} + \Gamma_{GE} H_{\ell,sat} + Q_E + \frac{S}{A}(m_D H_E - m_E H_F) \quad .$$

Table 2 Hydrodynamic Constitutive Equations

Wall-liquid drag force

$$\tau_{WF} = \bar{A}_{WF}\, f_{WF}\, \frac{\rho_F}{2}\, u_F\, u_F \text{ , in Pa/m}$$

f_{WF} = Blasius' expression

$$= \frac{1}{4}\left(\frac{0.316}{Re_F^{0.25}}\right), \text{ dimensionless}$$

Vapor-liquid drag force

$$\tau_{FG} = \bar{A}_{FG}\, f_{FG}\, \frac{\rho_G}{2}\, (u_G - u_F)\, u_G - u_F$$

f_{FG} = Wallis' expression

$$= \frac{1}{4}\left(\frac{0.316}{Re_G^{0.25}}\right)\left(1 + 300\, \frac{t_F}{D}\right)$$

Vapor-droplet drag force

$$\tau_{EG} = \bar{A}_{EG}\, K_{EG}\, \frac{\rho_G}{2}\, (u_G - u_E)\, u_G - u_F$$

$$K_{EG} = \frac{24}{Re_E}\left(1 + 0.15\, Re_E^{0.687}\right) + \frac{0.42}{1 + 4.25\times10^4\, Re_E^{-1.16}}$$

Droplet size

$$\delta_E = \begin{cases} \dfrac{\sigma\, We}{\rho_G (u_G - u_E)^2} \\ 10^{-3}, \text{ if } \delta_E < 10^{-3} \end{cases}$$

where We = Weber number (= 5)

Table 3 Summary of Experimental Conditions for Film Flow Measurements with Steam-Water in Tubes

Reference	Test Section inside Dia. mm	Number of Exp.	Test Conditions	Pressure MPa	Mass Flux kg/m^2s
Hewitt and Pulling[19]	9.3ϕ	67	Adiabatic	0.24-0.45	298
Keeys, Ralph and Roberts[20]	12.7ϕ	21	Adiabatic	3.4-6.9	1313-2765
Yanai[23]	12.0ϕ	23	Adiabatic	0.34	139-278
Würtz[3]	10.0ϕ	81	Adiabatic	3.0-9.0	500-3000
Würtz[3]	20.0ϕ	21	Adiabatic	7.0	500-2000

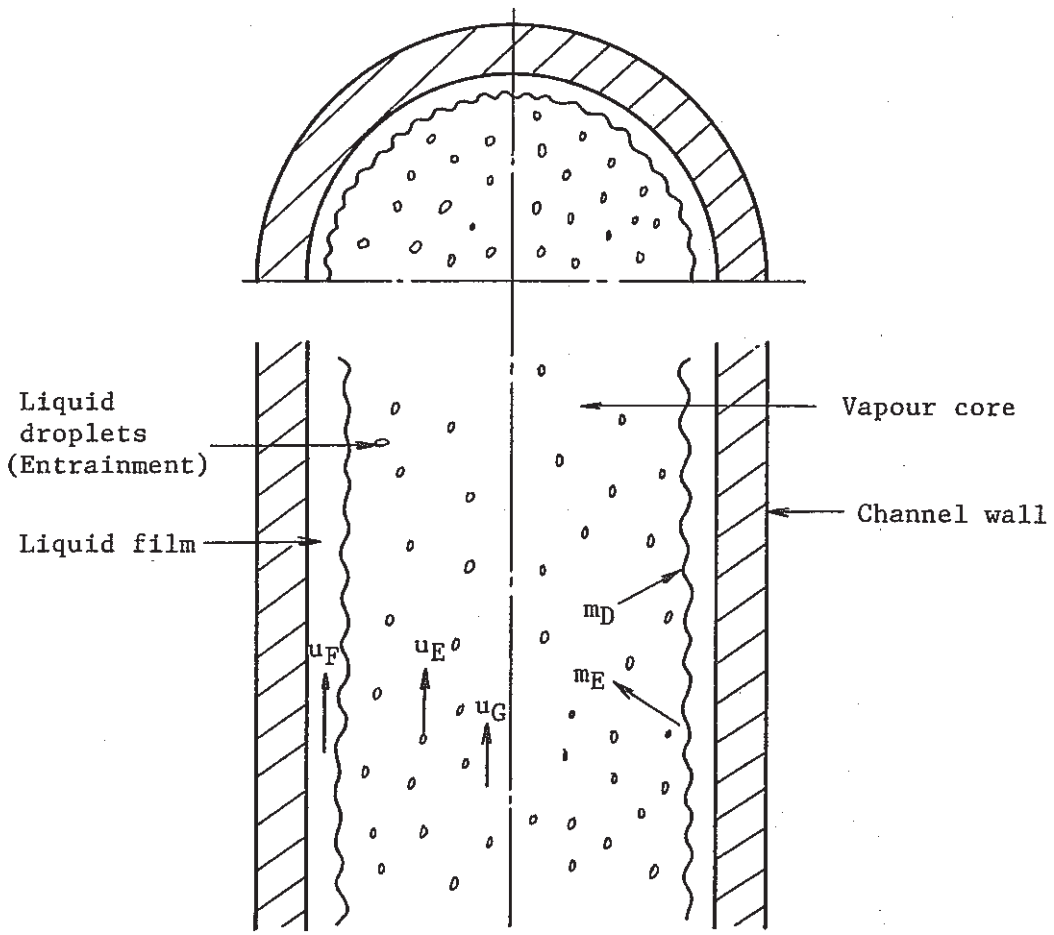

Fig. 1 Three-Fluid Modeling in Annular Two-Phase Flow

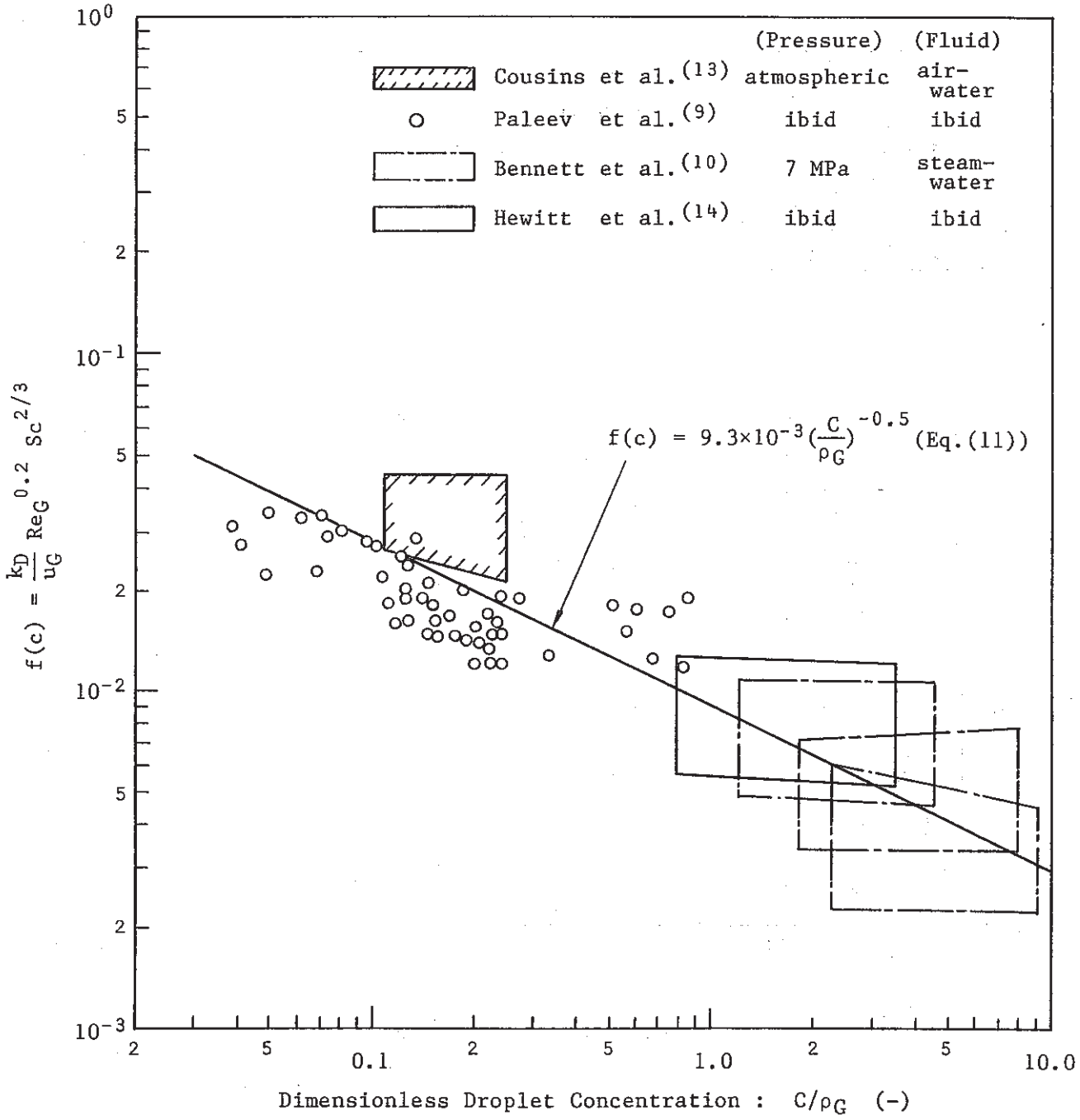

Fig. 2 Comparison of Deposion Model with Experimental Data

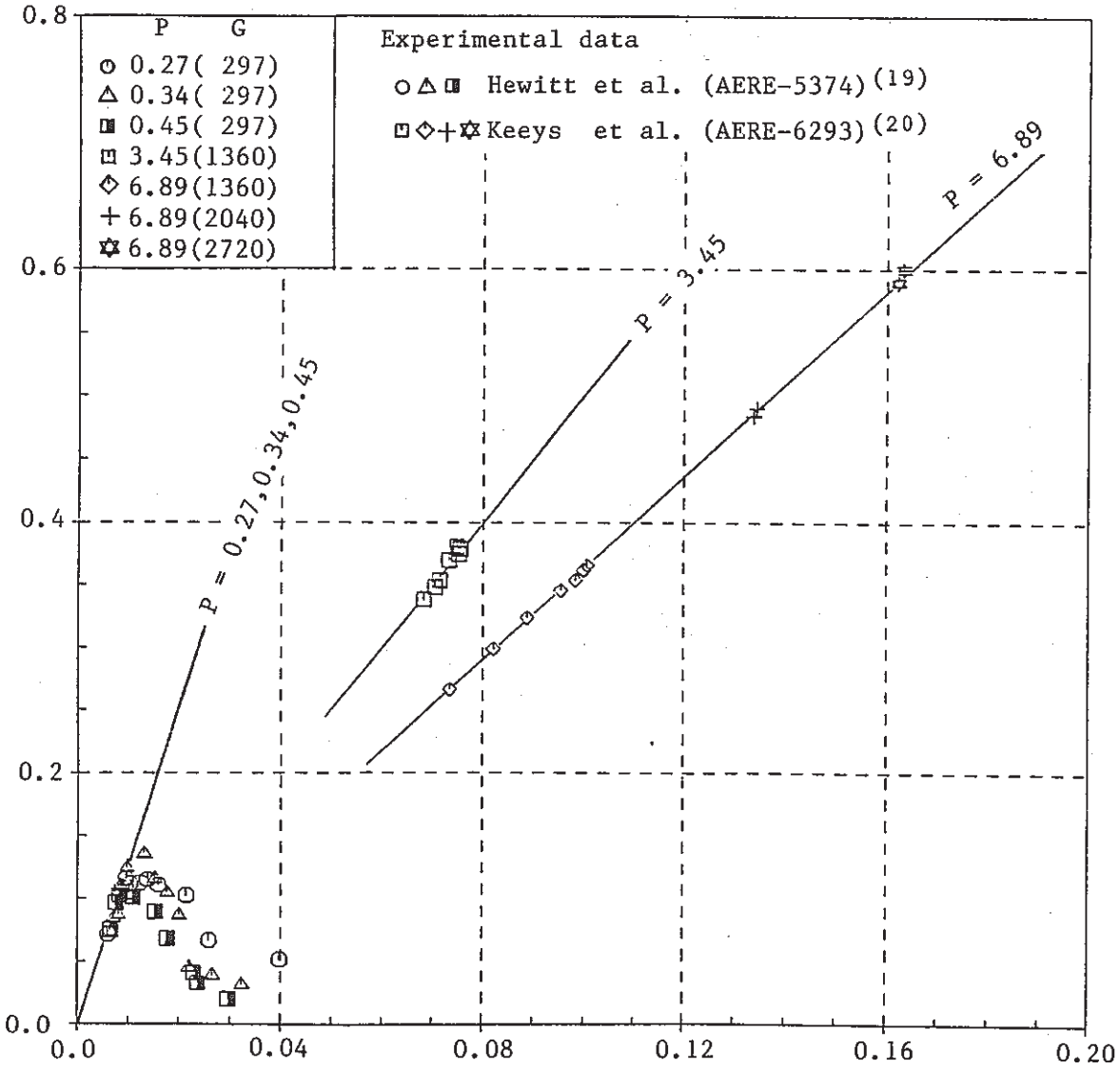

Fig. 3 Dimensionless Parameter(S_2) vs. Entrainment Rate

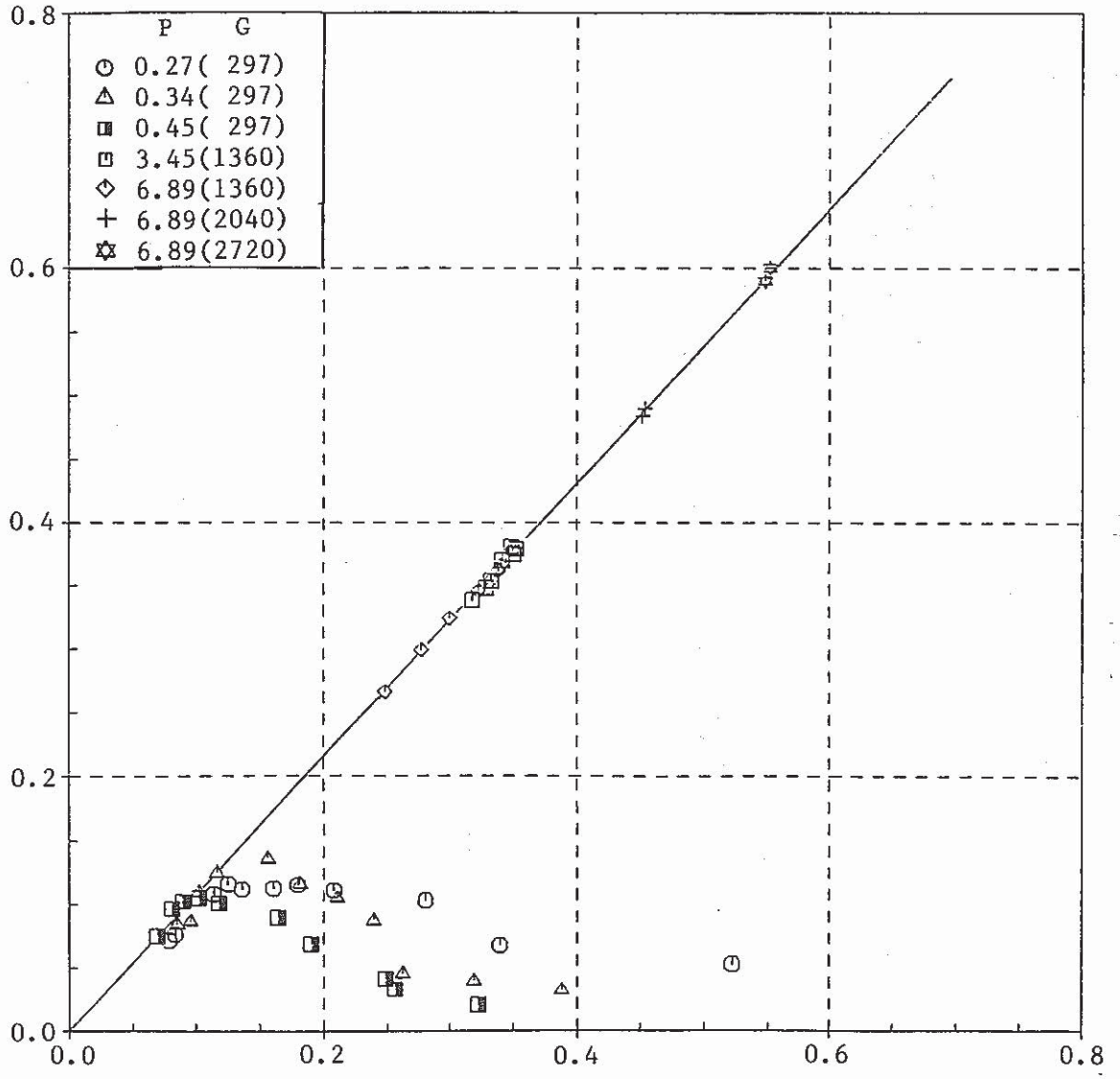

$$S_R = S_2 \left(\frac{\rho_F}{\rho_G}\right)^{0.40} = \left(\frac{\tau_{FG}\ \Delta h_{eq}}{\sigma}\right)\left(\frac{u_G\ \mu_F}{\sigma}\right)\left(\frac{\rho_F}{\rho_G}\right)^{0.40}$$

Fig. 4 Dimensionless Parameter(S_R) vs. Entrainment Rate

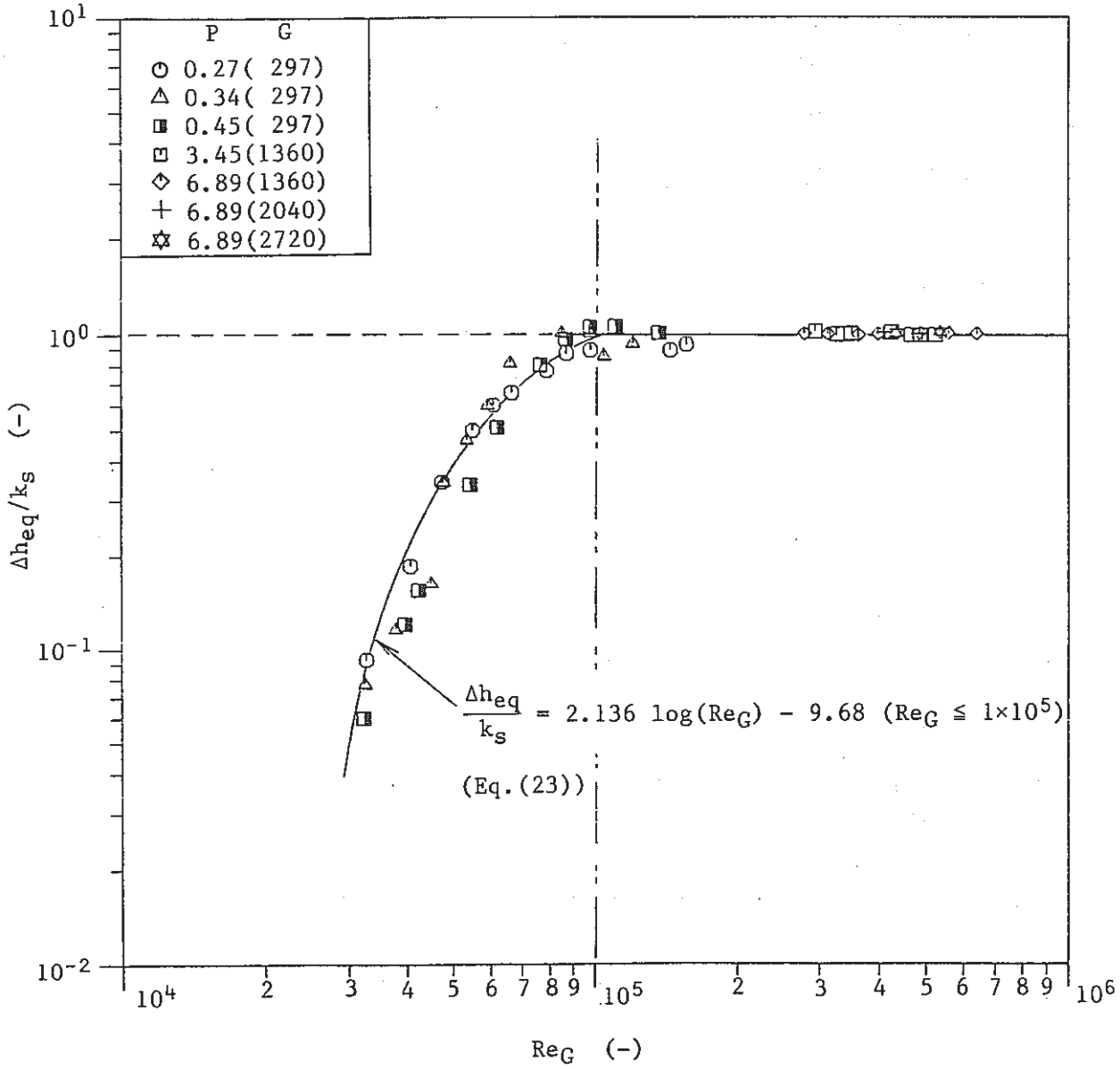

Fig. 5 Equivalent Height of Roll Wave vs. Gas Reynolds Number

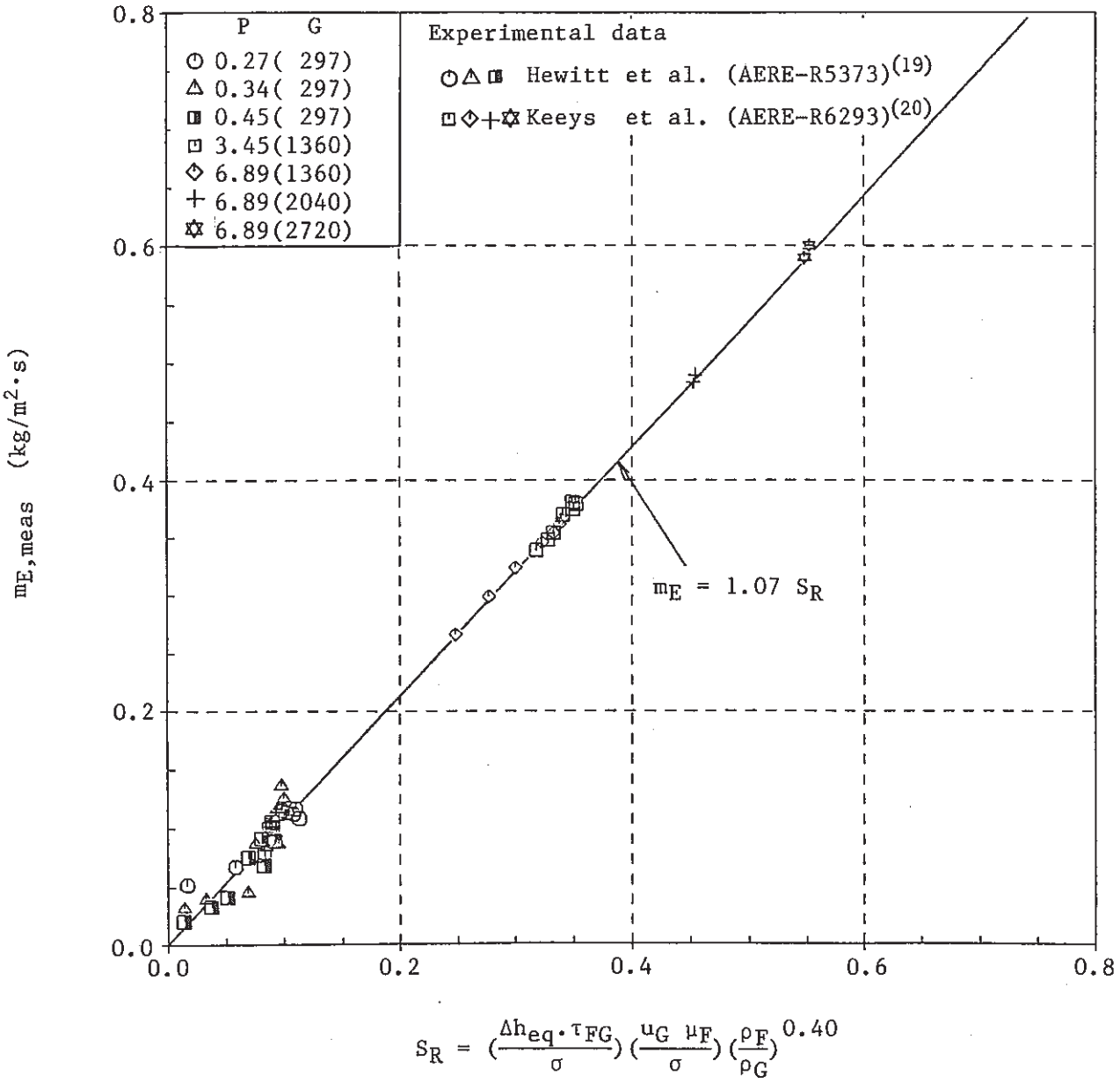

Fig. 6 Dimensionless Parameter S_R vs. Entrainment Rate Data

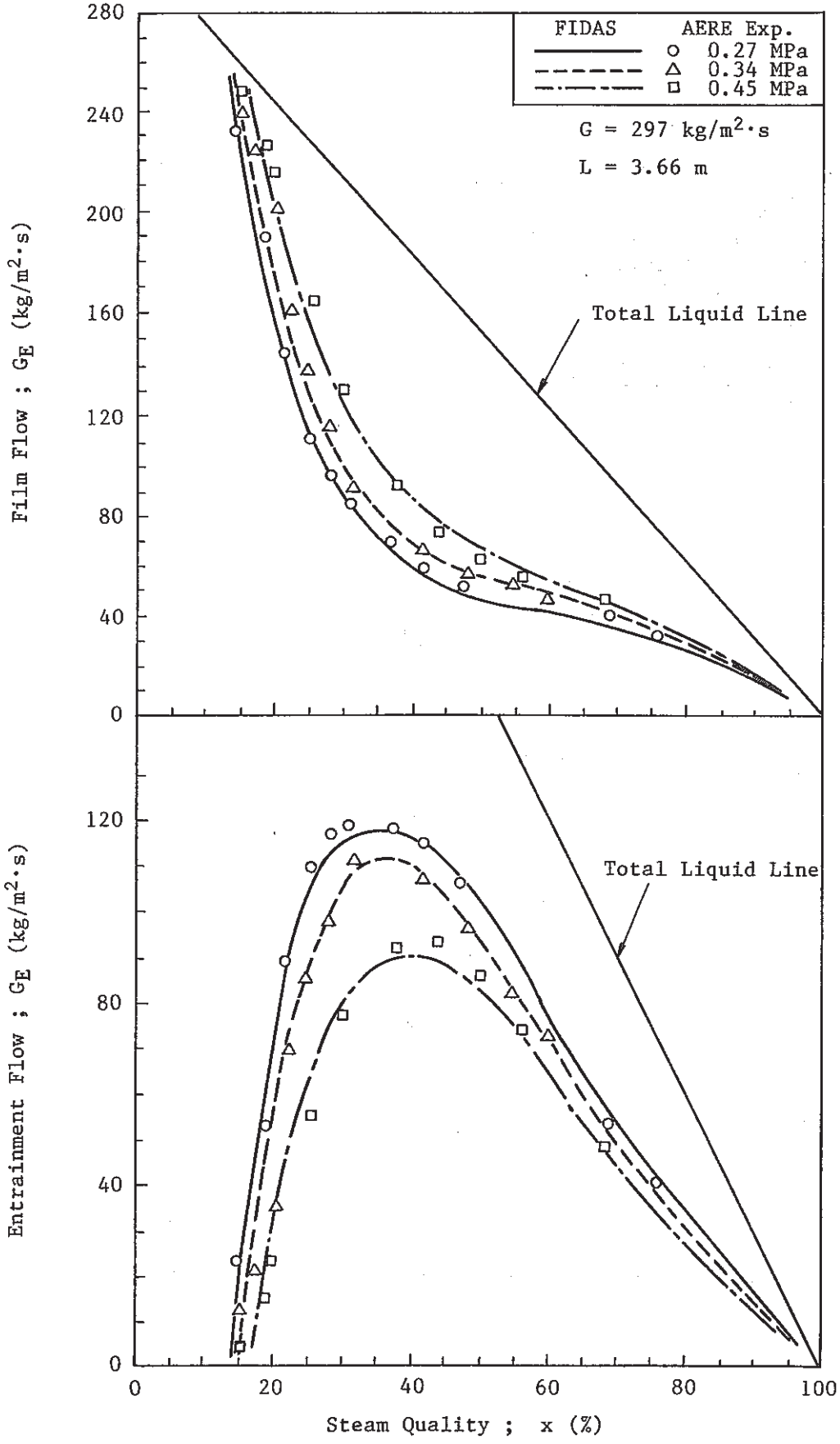

Fig. 7 Comparison between Analysis and Experiment of Hewitt et al.[19]

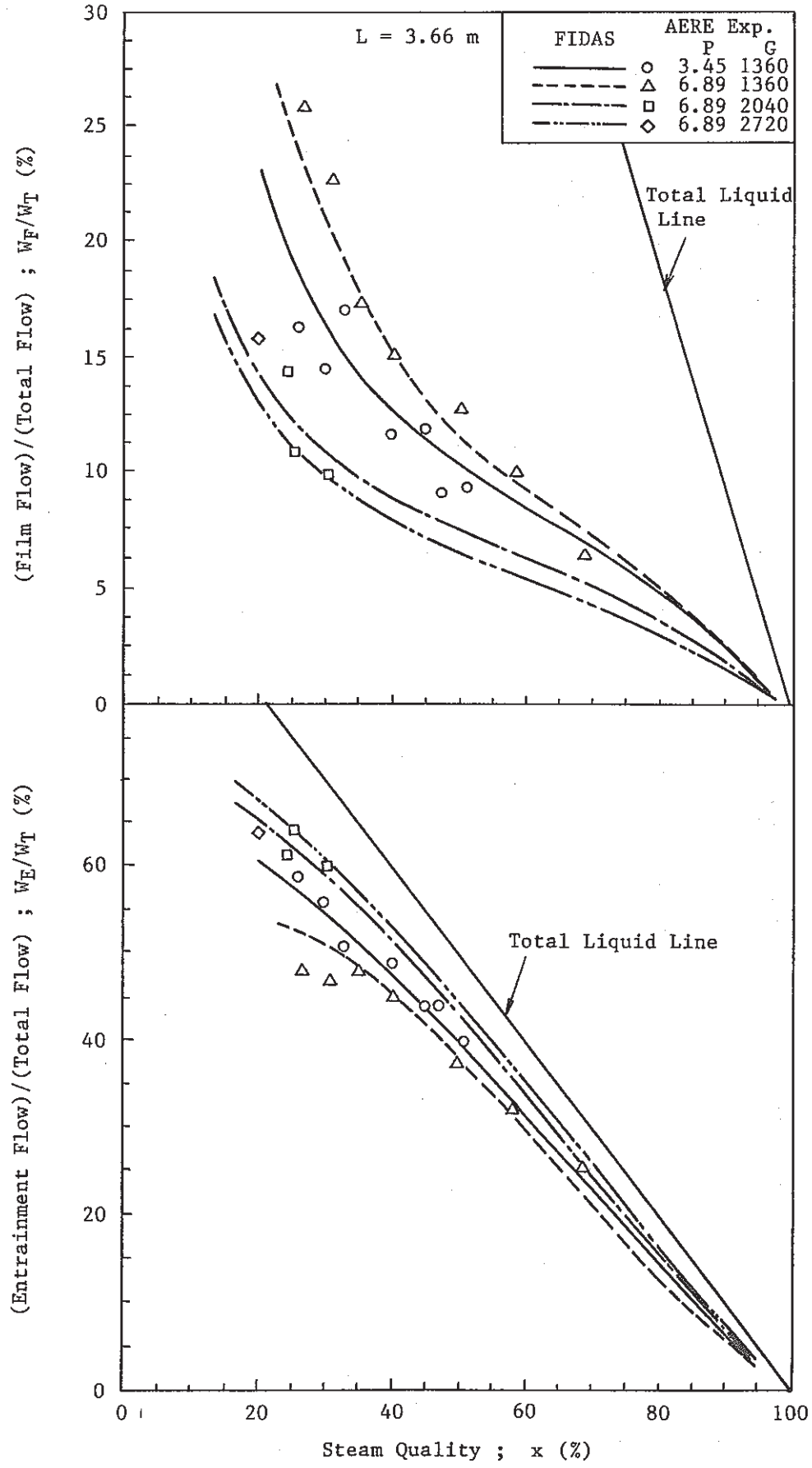

Fig. 8 Comparison between Analysis and Experiments of Keeys et al.[20]

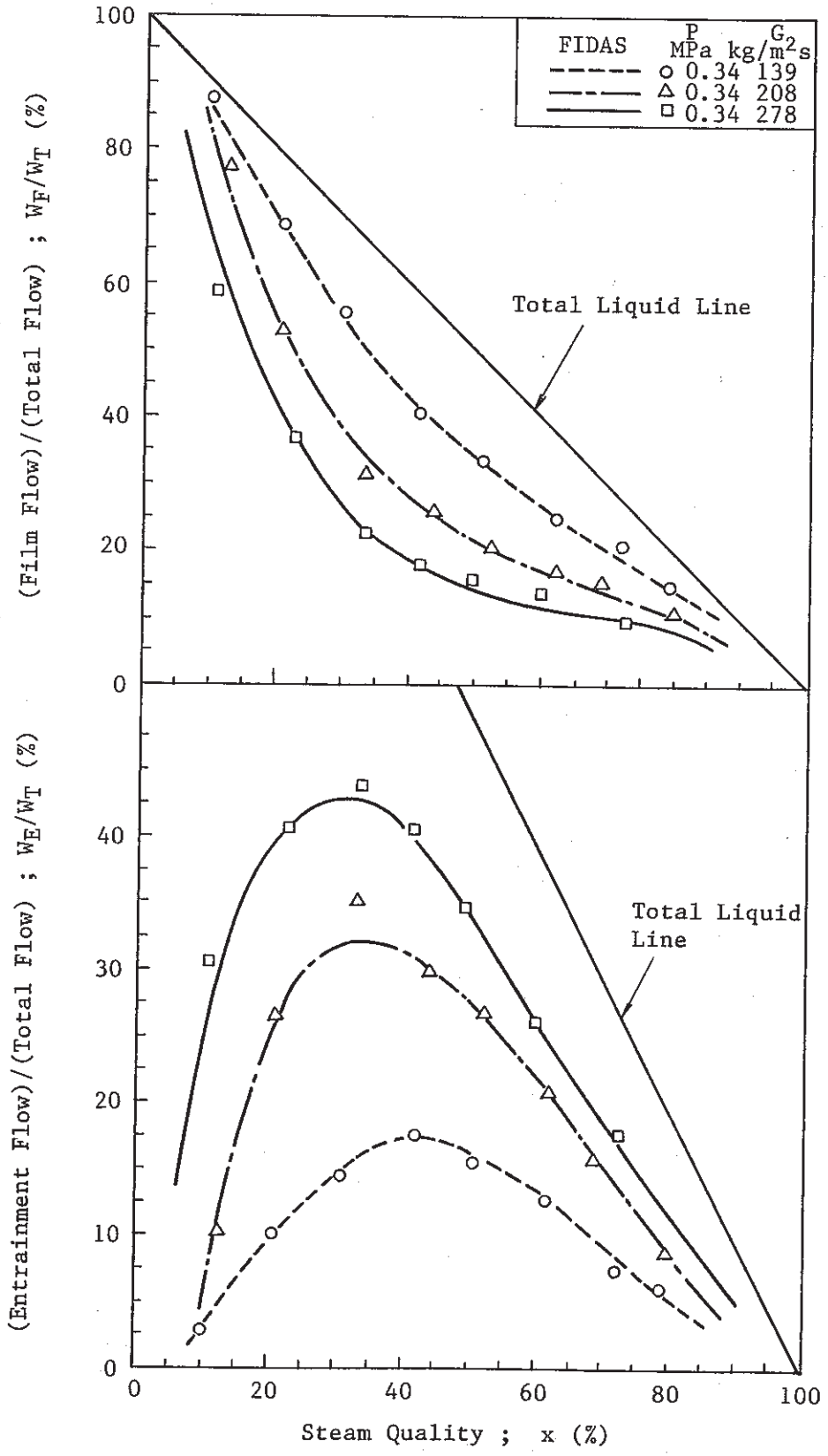

Fig. 9 Comparison between Analysis and Experiment of Yanai[23]

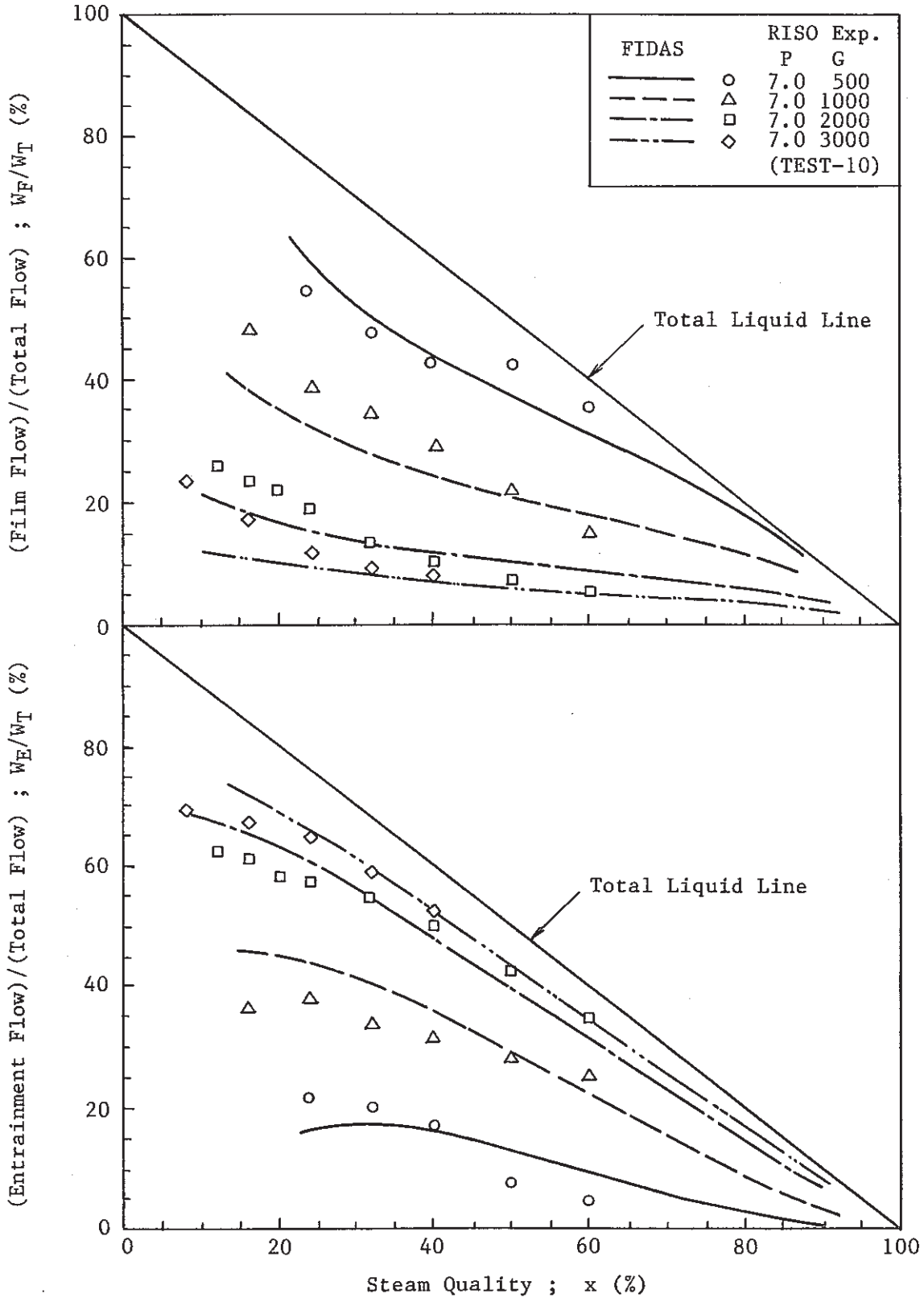

Fig. 10 Comparison between Analysis and Experiment of Wurtz[3] (D = 0.010 m)

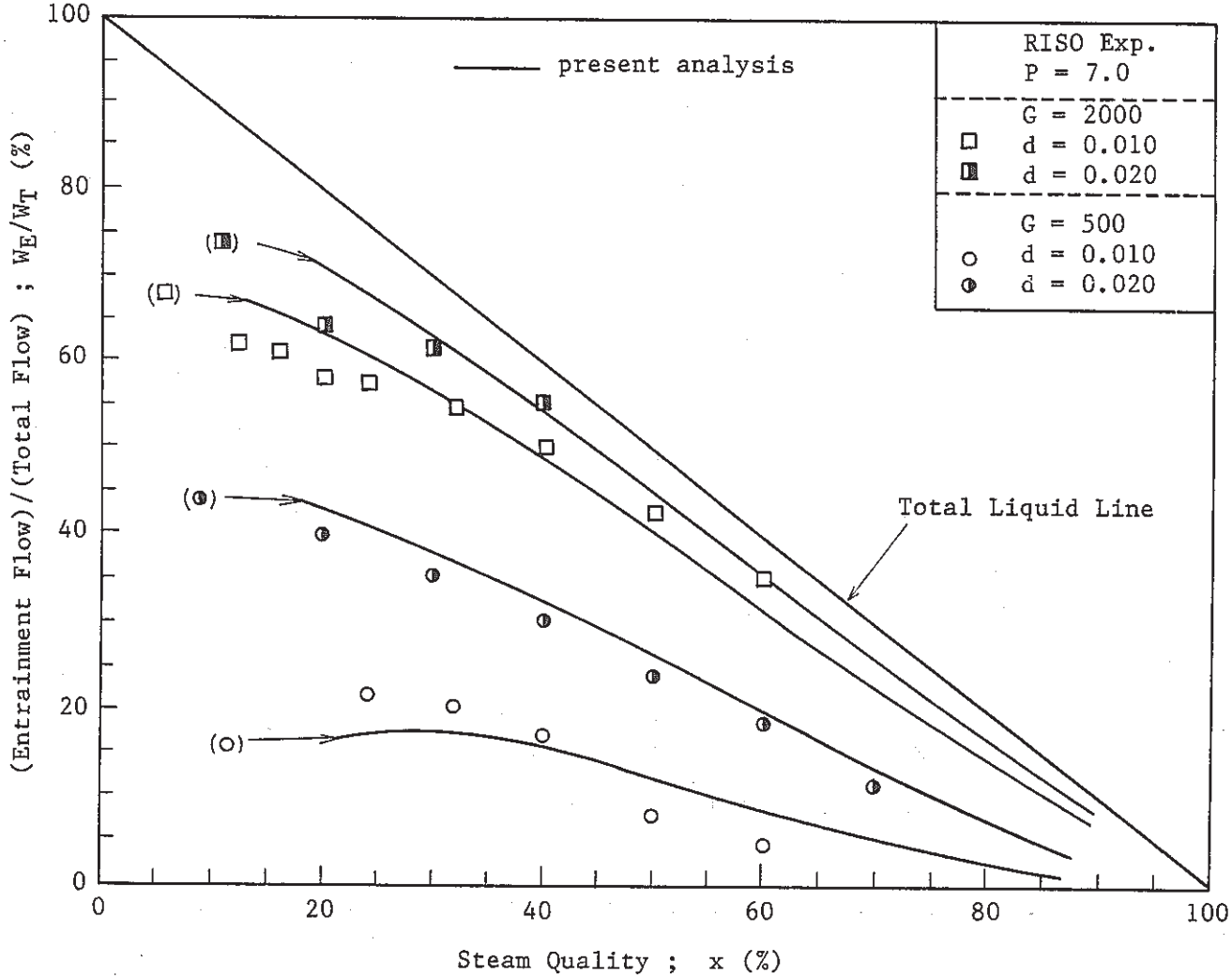

Fig. 11 Comparison between Analysis and Experiment of Wurtz[3]